Simultaneous B1 and T1 mapping based on modified "Actual Flip-angle Imaging"

T. Voigt[1], U. Katscher[2], K. Nehrke[2], and O. Doessel[1]

[1]Institute of Biomedical Engineering, University of Karlsruhe, Karlsruhe, Germany, [2]Philips Research Europe, Hamburg, Germany

Introduction: This abstract presents a new approach towards a fast, simultaneous B_1 and T_1 mapping technique. This is especially important due to the mutual dependency of these parameters. The new method is based on the "actual flip angle imaging" (AFI) sequence [1], however, using multiple TR pairs instead of the standard AFI approach of a single TR pair. In the following, this multiple TR method is called "MTR".

Theory: The standard AFI dual TR sequence is shown in Fig 1. The signal intensities S_1 and S_2 measured in the intervals TR_1 and TR_2, respectively, depend in general on various parameters. Solving the Bloch equation for the steady state assuming perfect spoiling of transverse magnetization yields the following structure:

$$S(TR_1, TR_2, TE, T_2^*; T_1, \alpha, \tilde{M}_0) = M_0(T_2^*, TE, \tilde{M}_0) \cdot F_i(TR_1, TR_2, \alpha, T_1) \quad (1),$$

with F_i being different for signals S_1 and S_2. For the first image S_1 it is found that:

$$F_1(\alpha, T_1) = ((1-E_2)\sin\alpha + \tfrac{1}{2}(1-E_1)E_2 \sin 2\alpha)/(1-E_1E_2\cos^2\alpha) \quad (2),$$

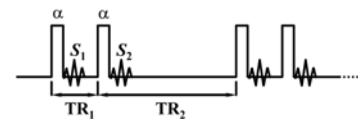

Figure 1: Dual TR sequence [1].

with $M_0 = \tilde{M}_0 \cdot e^{-TE/T_2^*}$ and $E_{1,2} = e^{-TR_{1,2}/T_1}$. S_2 can be obtained from (2) by interchanging indices. The AFI approach suggests dividing the two signals in order to remove M_0. Then, T_1 is neglected assuming $TR_i << T_1$, however, producing a systematic error. The MTR approach on the other hand employs multiple dual TR sequences in subsequent measurements. Each dual TR sequence gives two data points $F(TR_1,TR_2,\alpha,T_1)$ and $F(TR_2,TR_1,\alpha,T_1)$ from signals S_1 and S_2 for each pixel, yielding a total of $D = \{F(TR_i,TR_j,\alpha,T_1), F(TR_j,TR_i,\alpha,T_1) \,|\, i,j \in I_{MTR}\}$ for all TR combinations i,j used. The parameters α, T_1, and M_0 can then be obtained by a non-linear numerical fit of the theoretical expressions for the signal intensities (1,2) to the set of measured data points D. Hereby, α and T_1 are obtained simultaneously and independently of each other. Thus, no further correction of either parameter has to be made, and no systematic B_1/T_1 errors are present in this method.

Subjects and methods: 1: Simulations have been conducted to evaluate the noise behaviour of MTR B_1T_1 mapping in comparison to AFI mapping. Noise has been added to the signals (1,2), which then were used for reconstruction via AFI and MTR. 2: Experiments were carried out with the body coil of a 1.5T Achieva system (Philips Medical Systems, Best, The Netherlands). A phantom consisting of 6 compartments with different T_1 values was used. To obtain an independent reference to the MTR results, T_1 was additionally measured via RLSQ (combined SE + IR sequence [2]) with TR_SE / TR_IR = 1300 / 3500 ms, ΔTE = 50 ms, and 8 echoes. Three TR_1, TR_2 combinations with a nominal flip angle α=50° have been employed for MTR: TR_1 / TR_2 =50 / 200 ms, 50 / 250 ms, 50 / 300 ms. A 3D volume containing 30 slices (5 mm thickness), FOV 150×220 mm², spatial scan resolution 96×98 pixels, TE=1.72 ms has been acquired. For comparison of the flip angle results, a standard AFI image using TR_1=50 ms and TR_2=250 ms, α=50° and the same geometrical configuration was obtained. 3: Experiments on healthy volunteers were conducted with a 1.5T head coil, a nominal flip angle α = 50°, a spatial resolution of 1.25×1.25 mm², and 19 slices (12 mm thickness). Subsequent dual TR sequences were applied with TR_1 / TR_2= 40 / 80ms, 40 / 200 ms, and 40 / 400 ms. In all three cases (simulation, phantom, and *in vivo*), the reconstruction was performed using in-house C++-software based on the Gnu Scientific Library [3] implementation of Levenberg-Marquardt algorithm [4, 5].

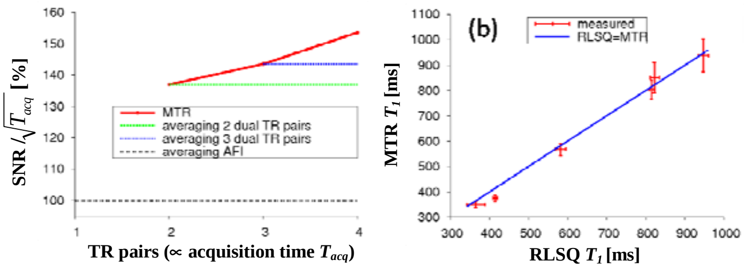

Figure 2: **Noise behaviour of MTR and AFI (a). SNR is shown normalized by square root of imaging time. (b): T_1 values obtained via MTR and RLSQ. All data points are close to the blue line, indicating good agreement.**

Results/Discussion: It can be deduced from simulations (Fig. 2a) that MTR is able to increase SNR by up to 53% compared to averaged AFI results. Thus, instead of averaging AFI data, additional scan time should be used for multiple TR pairs and reconstruction via the proposed MTR method. Quantitative T_1 estimation via MTR in the phantom is shown and evaluated in Fig. 2b, revealing good agreement to RLSQ results. B_1 results are shown in Fig. 3. Even in the case of sufficient spoiling [6], differences in the flip angle maps of MTR and AFI are obtained due to the systematic error in the AFI approach as a result of neglecting T_1 effects (Fig. 3c). Data points in the plots were obtained by averaging areas inside the tubes and on the background. Fig. 4 shows MTR *in vivo* B_1 and T_1 maps of high accuracy. MTR also seems less prone to (spoiling) artefacts (Fig. 4c).

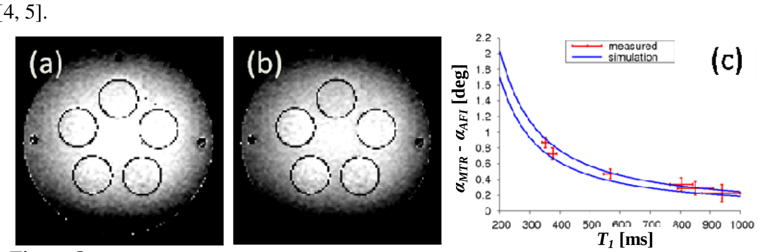

Figure 3: **Comparison of B_1 mapping via MTR (a) and AFI (b). (c): The flip angle differences between MTR and AFI observed in the experiment (red) agree with corresponding simulations (blue). The upper curve represents a nominal flip angle of α=50°, the lower curve α=45°, which corresponds to the range of actual flip angles observed in the experiment.**

Conclusion: In terms of accuracy and signal to noise ratio, the presented MTR B_1 mapping seems to outperform standard AFI. T_1-corrected B_1 maps of high accuracy and / or high resolution and / or short acquisition time are required, e.g., for conductivity imaging / local SAR determination [7]. Also parallel transmission like RF shimming [8] or Transmit SENSE [9] might benefit from MTR. On the other hand, the simultaneously obtained, B_1-corrected T_1 mapping could be used in the framework of quantitative MRI, e.g., the determination of contrast agent concentrations.

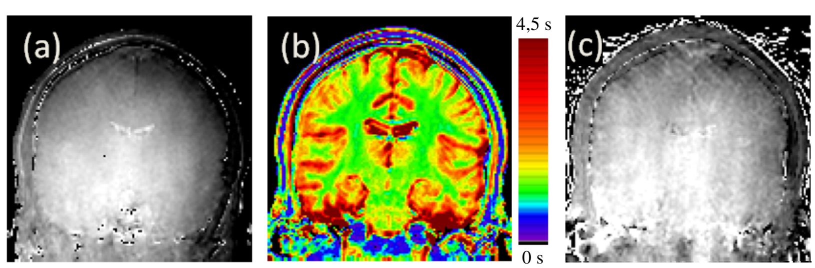

Figure 4: **MTR B_1 map of high accuracy (a). Good white and grey matter contrast is observed in the MTR T_1 map (b). (c) shows a standard AFI B_1 map, revealing typical artefacts.**

References: [1] Yarnykh VL., MRM 57 (2007), 192-200. [2] In den Kleef JJ. et al., MRM 5 (1987), 513-524. [3] http://www.gnu.org [4] Marquardt D., J. Soc. Indust. Appl. Math., 11 (1963), 431-441. [5] Levenberg K., Quart. Appl. Math., 2 (1944), 164-168. [6] Nehrke K., ISMRM 16 (2008) 3144. [7] Katscher U. et al., ISMRM 16 (2008), 1191. [8] Ibrahim TS. et al., Magn Reson Imag. 18 (2000), 733-42. [9] Katscher U. et al., MRM 49 (2003), 144-150.